Anomalous Angular Dependence of the Dynamic Structure Factor near Bragg Reflections: Graphite

R. Hambach,[1,2,3] C. Giorgetti,[1,2] N. Hiraoka,[4] Y. Q. Cai,[4,*] F. Sottile,[1,2] A. G. Marinopoulos,[5] F. Bechstedt,[3,2] and Lucia Reining[1,2]

[1]*Laboratoire des Solides Irradiés, Ecole Polytechnique, CEA/DSM, CNRS, 91128 Palaiseau, France*
[2]*European Theoretical Spectroscopy Facility (ETSF)*
[3]*Institut für Festkörpertheorie und -optik, Friedrich-Schiller-Universität Jena, 07743 Jena, Germany*
[4]*National Synchrotron Radiation Research Center, Hsinchu 30076, Taiwan*
[5]*CEMDRX, Department of Physics, University of Coimbra, P-3004-516 Coimbra, Portugal*

(Received 8 February 2008; published 31 December 2008)

The electron energy-loss function of graphite is studied for momentum transfers $\mathbf{q}$ beyond the first Brillouin zone. We find that near Bragg reflections the spectra can change drastically for very small variations in $\mathbf{q}$. The effect is investigated by means of first principle calculations in the random phase approximation and confirmed by inelastic x-ray scattering measurements of the dynamic structure factor $S(\mathbf{q}, \omega)$. We demonstrate that this effect is governed by crystal local field effects and the stacking of graphite. It is traced back to a strong coupling between excitations at small and large momentum transfers.

DOI: 10.1103/PhysRevLett.101.266406 PACS numbers: 71.45.Gm, 73.21.Ac, 78.70.Ck, 81.05.Uw

The momentum-resolved and frequency-dependent dynamic structure factor $S(\mathbf{q}, \omega)$ is a fundamental quantity in plasma physics, nuclear physics, particle physics, and condensed matter physics. It is important for the understanding of many problems like, e.g., electronic correlation, and it links the theory of many-body systems to scattering experiments like electron energy-loss spectroscopy (EELS) or inelastic x-ray scattering (IXS).

EELS measurements are particularly efficient for moderate momentum transfer, i.e. when $\mathbf{q}$ is shorter than a reciprocal-lattice vector and multiple scattering effects remain secondary. Recently, modern synchrotron radiation sources have opened the way to study electronic excitations at large momentum transfer using IXS [1,2]. New phenomena can be observed in this range, such as a periodic plasmon dispersion in magnesium diboride MgB_2 [2] or plasmon-bands in Silicon [3]. Crystal local field effects (LFE) [4,5], namely, the fact that an external perturbation can induce a response on the length scale of the structure of the material, become increasingly important for large $\mathbf{q}$ [6]. They acquire particular importance for layered systems, such as graphite [7], or superlattices [8].

Graphite, with its well separated and polarizable graphene sheets, is a very good candidate for the exploration of LFE-induced phenomena. EELS and IXS measurements (see, e.g., [1,9–11]) have determined the energy-loss spectra and plasmon dispersion for a wide range of momentum transfer $\mathbf{q}$. Calculations of the energy-loss function that are based on the homogeneous electron gas (see, e.g., [12–14]) or the tight-binding model (see, e.g., [15,16]) have been used extensively to study in-plane properties of graphite. *Ab initio* calculations based on Density-Functional Theory (DFT) in its time-dependent extension (TDDFT) [17], either in the adiabatic local density approximation (TDLDA) or even in the Random Phase Approximation (RPA), reproduce experimental plasmon spectra with very good precision [7,11] and show a continuous angular dependence of the dynamic structure factor for relatively moderate momentum transfer $\mathbf{q}$. The range of larger $\mathbf{q}$, instead, is much less explored.

In the present Letter, we demonstrate that this range offers access to striking phenomena. In particular, our *ab initio* calculations and IXS measurements reveal an anomaly in the angular dependence of the dynamic structure factor: For a momentum transfer close to certain reciprocal-lattice vectors, we observe drastic changes in the spectra upon small variations in $\mathbf{q}$. This discontinuous behavior should have important implications for the interpretation of measurements close to Bragg reflections in any strongly inhomogeneous system.

We performed first principle RPA calculations of the momentum-resolved and frequency-dependent dynamic structure factor $S(\mathbf{q}, \omega)$, which is directly related to the energy-loss function. The electronic ground state of graphite (Bernal stacking) was calculated in DFT-LDA (local density approximation) with ABINIT [18], using a plane-wave basis set [19] and norm-conserving pseudopotentials [20]. The Kohn-Sham band structure was used to compute the independent particle polarizability χ^0 with the DP-code [21]. In RPA, the longitudinal dielectric function ϵ and its inverse ϵ^{-1}, that links the total to the external potential in linear response $\varphi_{\text{tot}} = \epsilon^{-1}\varphi_{\text{ext}}$ is given by $\epsilon = 1 - v\chi^0$, where v denotes the Coulomb interaction. For a solid, ϵ is a *matrix* in reciprocal-lattice vectors $(\mathbf{G}, \mathbf{G}')$ and a function of the reduced momentum transfer $\mathbf{q}_r$ inside the first Brillouin zone and of frequency ω. The dynamic structure factor for a given momentum transfer $\mathbf{q} = \mathbf{q}_r + \mathbf{G}_0$ and frequency ω is then

$$S(\mathbf{q},\omega) = -\frac{q^2}{4\pi^2 n_0}\,\mathrm{Im}[\epsilon^{-1}_{\mathbf{G}_0\mathbf{G}_0}(\mathbf{q}_r,\omega)];$$

where $\mathbf{G}_0$ is a reciprocal-lattice vector and n_0 denotes the average electron density. Hence, only diagonal elements of ϵ^{-1} are needed. However, as ϵ is *not* diagonal for an inhomogeneous material, its inversion will mix all matrix elements. One can understand the physics of this mathematical fact by expanding $\epsilon^{-1} = (1 - v\chi^0)^{-1}$:

$$\epsilon^{-1}_{\mathbf{G}_0\mathbf{G}_0}(\mathbf{q}_r,\omega) = 1 + v_{\mathbf{G}_0}\chi^0_{\mathbf{G}_0\mathbf{G}_0}(\mathbf{q}_r,\omega) + \sum_{\mathbf{G}} v_{\mathbf{G}_0}\chi^0_{\mathbf{G}_0\mathbf{G}}(\mathbf{q}_r,\omega)v_{\mathbf{G}}\chi^0_{\mathbf{G}\mathbf{G}_0}(\mathbf{q}_r,\omega) + \ldots.$$

The first order term gives the response of the independent particles to the external potential. The second term is the response to the Hartree potential that is induced by the first order response. This self-consistent process is then continued to infinite order. As χ_0 is a matrix, an external potential with momentum $\mathbf{q}_r + \mathbf{G}_0$ can induce spatial charge fluctuations, whose momentum $\mathbf{q}_r + \mathbf{G}$ differs by any reciprocal-lattice vector, and to which the system will *also* respond; these are the (crystal) LFE.

When $\mathbf{q} = \mathbf{q}_r$ is small, all induced potentials are of shorter wavelength, i.e., $|\mathbf{G}| > |\mathbf{G}_0|$. However, for large $\mathbf{q} = \mathbf{q}_r + \mathbf{G}_0$ beyond the first Brillouin zone, long wavelength fluctuations with $|\mathbf{G}| < |\mathbf{G}_0|$ may be induced, too. They have been found to cause a Fano resonance in silicon [22] and lithium [23] and a periodic plasmon dispersion in magnesium diboride MgB_2 [2]. We will now show that the situation is particularly striking for graphite, where the long wavelength fluctuations give rise to an unexpected discontinuity in the dynamic structure factor.

Figure 1(a) shows the calculated dynamic structure factor $S(\mathbf{q},\omega)$ of graphite for a sequence of $\mathbf{q} = (0, 0, q_3)$ that are chosen exactly perpendicular to the planes [Note that $(q_1, q_2, q_3) = q_1\mathbf{b}_1 + q_2\mathbf{b}_2 + q_3\mathbf{b}_3$ where the $\mathbf{b}_n$ are primitive reciprocal-lattice vectors; see Fig. 3(b)]. The structures that can be seen in this low-energy range are due to the very weak interaction between the graphene sheets; the intensity of the spectrum is therefore quite low and the dispersion small, contrary to the case of MgB_2 [2] where the coupling between layers is much stronger.

Instead, Fig. 1(b) shows calculations for momentum transfers $\mathbf{q} = (\frac{1}{8}, 0, q_3)$ where the in-plane component $q_1 = \frac{1}{8}$ is kept fixed and the perpendicular component q_3 is varied. Although for large q_3 the direction of $\mathbf{q}$ deviates only slightly from the c-axis, we observe a striking difference compared to the on-axis results: First, the intensity is significantly increased for most of the spectra—when q_3 is zero, we simply see the in-plane π-plasmon. Second, there is a strong dispersion in the peak positions; the main peak shifts between 7.6 eV at $q_3 = 0$ and 6 eV at $q_3 = 1$. The most striking observation, however, is the disappearance of the peak at $q_3 = 2$: for that value, the dynamic structure factor abruptly becomes completely flat below 8 eV. There

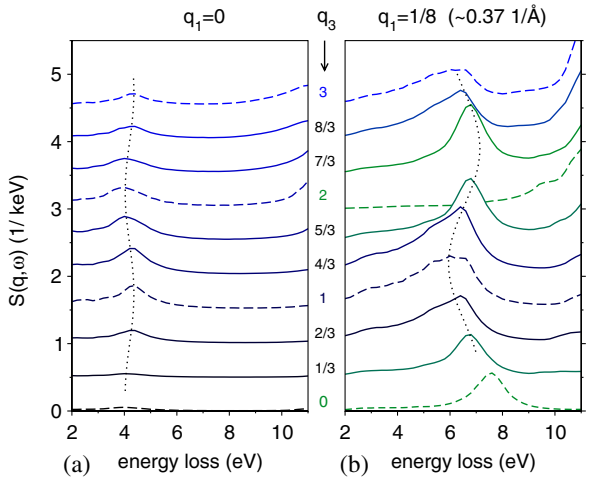

FIG. 1 (color online). Calculated dynamic structure factor $S(\mathbf{q},\omega)$ of graphite for different momentum transfers $\mathbf{q} = (q_1, 0, q_3)$ (a) exactly perpendicular to the planes ($q_1 = 0$) and (b) with a small in-plane component ($q_1 = \frac{1}{8}$). Dashed lines indicate spectra for integer q_3. All spectra have been shifted equidistantly in the y-direction for better visibility. Dotted lines are guides to the eye.

is hence a *significant* change of the spectra for a *small* change of $\mathbf{q}$. Even more important, these results remain valid for arbitrarily small in-plane components q_1, as we will see in the following.

The bottom panel of Fig. 2(a) shows $S(\mathbf{q},\omega)$ calculated with and without LFE (solid and dashed lines, respectively) for momentum transfers $\mathbf{q} = \boldsymbol{\eta}$ that are vanishingly small ($|\boldsymbol{\eta}| = 5 \times 10^{-5}$ Å^{-1}) and differ only in the angle α to the c-axis. For in-plane momentum transfers ($\alpha = 90°$), we find a pronounced π-plasmon peak at 7 eV, whereas in the perpendicular direction ($\alpha = 0°$), a peak, although of much lower intensity, is found at 4 eV. For intermediate directions of $\boldsymbol{\eta}$, one finds a continuous behavior when the angle α is changed, as one would expect. LFE contribute only marginally; i.e., the anisotropy simply stems from the anisotropy of the head element $\epsilon_{\mathbf{00}}(\boldsymbol{\eta},\omega)$ of the dielectric matrix. These results are consistent with earlier calculations on graphite [7].

Moving on to large momentum transfers, the next higher panel displays the results for $\mathbf{q} = (0, 0, 1) + \boldsymbol{\eta}$. A change in $\boldsymbol{\eta}$ corresponds now to an infinitesimal change in $\mathbf{q}$ [see Fig. 2(b)]. Only one spectrum is shown as it does not change with $\boldsymbol{\eta}$. It should be noted however that LFE start to become significant because of the larger $\mathbf{q}$.

This picture changes completely when we reach momentum transfers $\mathbf{q} = (0, 0, 2) + \boldsymbol{\eta}$ near the second reciprocal-lattice vector, shown in the top panel of Fig. 2(a): whereas the spectrum *without* LFE is completely flat and remains stable while $\boldsymbol{\eta}$ is changed, we find that LFE lead to drastic modifications of the spectra for infinitesimal variations of the total momentum transfer $\mathbf{q}$. A direct comparison between spectra for momentum transfers $\mathbf{q} = (0, 0, 2) + \boldsymbol{\eta}$ and the corresponding reduced mo-

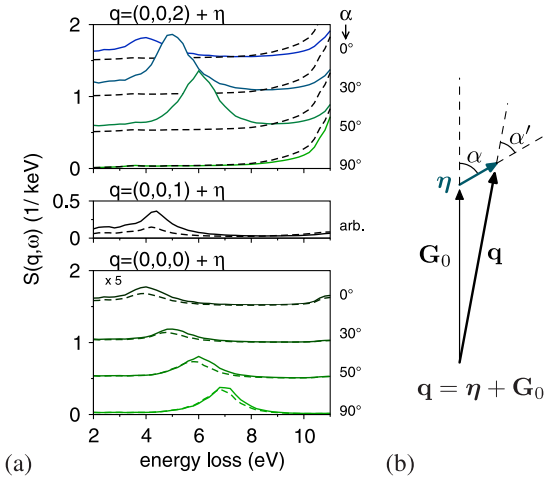

FIG. 2 (color online). (a) Dynamic structure factor $S(\boldsymbol{\eta} + \mathbf{G}_0, \omega)$ for small deviations $|\boldsymbol{\eta}| = 5 \times 10^{-5}$ Å^{-1} from reciprocal-lattice vectors $\mathbf{G}_0$ calculated with (solid line) or without (dashed line) LFE. (Bottom) For $\mathbf{G}_0 = (0, 0, 0)$, $S(\boldsymbol{\eta}, \omega)$ depends on the direction of $\boldsymbol{\eta}$. (Middle) For $\mathbf{G}_0 = (0, 0, 1)$, arbitrary $\boldsymbol{\eta}$ lead to the same spectrum. (Top) For $\mathbf{G}_0 = (0, 0, 2)$, $S(\boldsymbol{\eta} + \mathbf{G}_0, \omega)$ again changes with $\boldsymbol{\eta}$, but only when LFE are included. (b) Definition of the angles α and α'.

mentum transfer $\boldsymbol{\eta}$ (top vs bottom panel) shows that they are very similar up to a scaling factor, whenever $\boldsymbol{\eta}$ is not exactly in-plane. In other words, near the reciprocal-lattice vector (0, 0, 2), LFE lead to the reappearance of spectra of lower Brillouin zones [2,22], and the dynamic structure factor is determined by the direction of the *reduced* momentum transfer $\mathbf{q}_r = \boldsymbol{\eta}$ and *not* by the direction of $\mathbf{q}$.

Graphite is a very convenient case for further analysis because for small $\mathbf{q}_r$ and $\mathbf{G}_0 = (0, 0, 2)$, the coupling element $\epsilon_{\mathbf{0G}_0}(\mathbf{q}_r, \omega)$ dominates by far all other off-diagonal elements $\epsilon_{\mathbf{GG}'}(\mathbf{q}_r, \omega)$. Neglecting the latter, the inversion of ϵ reduces to the inversion of a simple 2×2 dielectric matrix [24] and one obtains (the ω dependence is omitted)

$$\epsilon^{-1}_{\mathbf{G}_0\mathbf{G}_0}(\mathbf{q}_r) = \frac{1}{\epsilon_{\mathbf{G}_0\mathbf{G}_0}(\mathbf{q}_r)} + \frac{\epsilon_{\mathbf{G}_0\mathbf{0}}(\mathbf{q}_r)\epsilon_{\mathbf{0G}_0}(\mathbf{q}_r)}{[\epsilon_{\mathbf{G}_0\mathbf{G}_0}(\mathbf{q}_r)]^2}\,\epsilon^{-1}_{\mathbf{00}}(\mathbf{q}_r).$$

This result is similar to the two-plasmon-band approximation [25]. The first term corresponds to the result without LFE. The second term leads to the reappearance of the spectrum $\epsilon^{-1}_{\mathbf{00}}(\mathbf{q}_r, \omega)$ weighted by the coupling element. Whenever the second term is strong, the spectrum for large $\mathbf{q} = \mathbf{q}_r + \mathbf{G}_0$ will also depend on the one for the reduced component $\mathbf{q}_r$, and hence on its anisotropy.

Still, it remains to be understood why this coupling to $\mathbf{q} \to \mathbf{0}$ appears *neither* for in-plane deviations $\mathbf{q} = (\eta, 0, 2)$, *nor* around $\mathbf{G}_0 = (0, 0, 1)$. To this end, we can make use of general properties of the dielectric function in semiconductors. In the limit of high frequencies, the coupling element can be approximated as [26]

$$\epsilon_{\mathbf{0G}_0}(\mathbf{q}_r, \omega) = \frac{4\pi}{\omega^2}\,\frac{\mathbf{q}_r \cdot (\mathbf{q}_r + \mathbf{G}_0)}{q_r^2}\,n(-\mathbf{G}_0),$$

where $n(-\mathbf{G}_0)$ denotes the Fourier coefficient of the electron density. A similar expression has been found by Sturm and Oliveira [25] in the framework of a quasifree electron gas. First, we see from this equation that the coupling between density fluctuations with momentum $\mathbf{q}_r$ and $\mathbf{q}_r + \mathbf{G}_0$ is proportional to the cosine of the enclosed angle α' [see Fig. 2(b)]. The prefactor $\epsilon_{\mathbf{G}_0\mathbf{0}}\epsilon_{\mathbf{0G}_0}/\epsilon^2_{\mathbf{G}_0\mathbf{G}_0} \propto \cos^2\alpha'$ enforces the anisotropy of the spectra: in particular, for a small in-plane $\mathbf{q}_r$, one has $\alpha = 90° \approx \alpha'$, which explains the absence of strong LFE in the spectrum for $\alpha = 90°$ [Fig. 2(a), top panel]. Second, the coupling element vanishes whenever the crystal structure factor, which is proportional to $n(-\mathbf{G}_0)$ becomes zero; i.e., whenever the Bragg reflection at $\mathbf{G}_0$ is forbidden. For graphite in Bernal stacking, this is the case for all $\mathbf{G}_0 = (0, 0, 2m + 1)$ where m is an integer. LFE around (0, 0, 1) stem hence only from a mixing with other *nonvanishing* $\mathbf{G} \neq \mathbf{0}$ beyond the 2×2 model. They do not introduce any significant dependence on the direction of $\mathbf{q}_r$ since $\mathbf{G} + \mathbf{q}_r \approx \mathbf{G}$. Instead, for $\mathbf{G}_0 = (0, 0, 2m)$, the two graphite planes A and B in the unit cell contribute in a constructive way (analogous to the constructive interference in the case of the Bragg reflection), which leads to the strong effect.

With these explanations in mind, let us come back to the results shown in Fig. 1(b). Since $\mathbf{q}_r$ is still reasonably small, the above arguments hold. In particular, we can explain the drastic spectral changes near (0, 0, 2) by the fact that (i) the spectrum from the first Brillouin zone reappears, which strongly depends on the direction of $\mathbf{q}_r$ (angle α) due to the anisotropy of graphite, and that (ii) the coupling and hence the strength of the recurring spectra is proportional to $|\mathbf{q}_r \cdot \mathbf{q}|^2 \propto \cos^2\alpha'$.

One may wonder whether such a spectacular effect can actually be observed, or whether it is masked either by

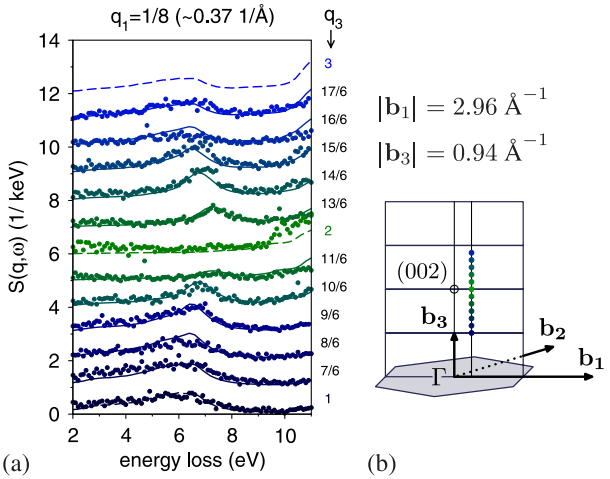

FIG. 3 (color online). (a) Comparison of the structure factor $S(\mathbf{q}, \omega)$ measured by IXS-experiments (dots) and calculated in RPA (lines; dashed for integer q_3) for $\mathbf{q} = (\frac{1}{8}, 0, q_3)$. The elastic tail has been removed from the raw experimental data and a uniform scaling has been applied. (b) Measured $\mathbf{q}$-points in reciprocal space.

exchange-correlation effects that are neglected in RPA, or by experimental conditions like a strong elastic tail near the Bragg reflection. Therefore, we have conducted inelastic x-ray scattering measurements for momentum transfers $\mathbf{q} = (\frac{1}{8}, 0, \frac{n}{6})$ covering the range between $\mathbf{q} = (0, 0, 1)$ and $(0, 0, 3)$. The in-plane component $|q_1 \mathbf{b}_1| = 0.37$ Å^{-1} is still small enough to create the desired effect [see Fig. 1(b)], but large enough to avoid the Bragg reflection. The measurements were carried out at the Taiwan inelastic scattering beam line in SPring-8 (BL12XU). The graphite sample was a plate having a surface of 2×3 mm^2 and a thickness of 100 μm [27]. The x-ray Laue photograph showed very nice spots, indicating that the sample was not Highly Oriented Pyrolitic Graphite but a single crystal. The energy resolution was 140 meV. A Si 400 four-bounce monochromator and a Si 444 spherical crystal analyzer were used. The momentum resolutions were approximately 0.15 Å^{-1} along the horizontal and the vertical axes. In order to subtract the tails of the elastic lines for the spectra, glass was measured as a reference. Figure 3(a) shows the measured spectra (dots) together with the corresponding calculated results (lines). The agreement is very good; in particular, the predicted peak shift is clearly seen in the measurements, as well as the abrupt change from a peaked spectrum for $\mathbf{q} = (\frac{1}{8}, 0, \frac{13}{6})$ to a completely flat one at $\mathbf{q} = (\frac{1}{8}, 0, 2)$, and the difference between $q_3 = \frac{13}{6}$ and $\frac{11}{6}$ due to the different angles α' [see Fig. 2(b)]. Hence, our measurements give unambiguous support to the presented theoretical predictions.

Beyond our studies of graphite, we expect similar results for other anisotropic crystals with strong LFE, especially for layered or quasi 1D structures. The exact reappearance of spectra from other Brillouin zones might however be obscured by the coupling factor, which is in general frequency dependent and complex valued, or the need to go beyond the two-plasmon-band approximation.

In conclusion, our RPA calculations and IXS measurements revealed and explained a striking discontinuity in the dynamic structure factor $S(\mathbf{q}, \omega)$ of graphite at momentum transfers $\mathbf{q}_r + \mathbf{G}_0$ close to Bragg allowed reciprocal-lattice vectors $\mathbf{G}_0$: infinitesimal changes in the momentum transfer induce strong changes in the resulting spectra. No discontinuity is observed when the crystal structure factor vanishes. It is hence a consequence of the Bernal stacking of the graphene layers that no changes occur at $\mathbf{G}_0 = (0, 0, 1)$. The theoretically predicted and experimentally observed effect has important consequences for measurements of $S(\mathbf{q}, \omega)$ close to an allowed Bragg reflection, as the resulting spectra can be *extremely sensitive* to the chosen momentum transfer. It is also an important step forward in the understanding of the dynamic structure factor of anisotropic systems, that may have broad implications including the description of strongly correlated systems.

This work was supported by the EU's FP7 through the ETSF-I3 project (Contract No. 211956) and by the ANR (Project NT05-3 43900). The experiment was carried out under an approval of SPring-8 and NSRRC (Proposal No. C04B12XU-1510N). Y. C. and N. H. are grateful to Professor Hiroyoshi Suematsu for providing us with the single crystal of graphite. R. H. thanks the Dr. Carl Duisberg-Stiftung and C'Nano IdF (IF07-800/R).

*Current address: National Synchrotron Light Source II, Brookhaven National Laboratory, Upton, NY 11973.

[1] N. Hiraoka *et al.*, Phys. Rev. B **72**, 075103 (2005).
[2] Y. Q. Cai *et al.*, Phys. Rev. Lett. **97**, 176402 (2006).
[3] W. Schülke and A. Kaprolat, Phys. Rev. Lett. **67**, 879 (1991).
[4] S. L. Adler, Phys. Rev. **126**, 413 (1962).
[5] N. Wiser, Phys. Rev. **129**, 62 (1963).
[6] S. Waidmann *et al.*, Phys. Rev. B **61**, 10149 (2000).
[7] A. G. Marinopoulos *et al.*, Phys. Rev. B **69**, 245419 (2004).
[8] S. Botti *et al.*, Phys. Rev. Lett. **89**, 216803 (2002).
[9] K. Zeppenfeld, Z. Phys. A **211**, 391 (1968).
[10] K. Zeppenfeld, Z. Phys. A **243**, 229 (1971).
[11] A. G. Marinopoulos *et al.*, Phys. Rev. Lett. **89**, 076402 (2002).
[12] P. B. Visscher and L. M. Falicov, Phys. Rev. B **3**, 2541 (1971).
[13] D. Grecu, Phys. Rev. B **8**, 1958 (1973).
[14] A. L. Fetter, Ann. Phys. (N.Y.) **88**, 1 (1974).
[15] C. S. Huang, M. F. Lin, and D. S. Chuu, Solid State Commun. **103**, 603 (1997).
[16] M. F. Lin, C. S. Huang, and D. S. Chuu, Phys. Rev. B **55**, 13961 (1997).
[17] E. Runge and E. K. U. Gross, Phys. Rev. Lett. **52**, 997 (1984).
[18] X. Gonze *et al.*, Comput. Mater. Sci. **25**, 478 (2002).
[19] We used 6144 *k*-points and an energy cutoff of 28 hartree.
[20] N. Troullier and J. L. Martins, Phys. Rev. B **43**, 1993 (1991).
[21] http://www.dp-code.org; V. Olevano *et al.* (unpublished).
[22] K. Sturm, W. Schülke, and J. R. Schmitz, Phys. Rev. Lett. **68**, 228 (1992).
[23] K. Höppner, A. Kaprolat, and W. Schülke, Eur. Phys. J. B **5**, 53 (1998).
[24] Indeed, we have verified that results of calculations neglecting all other off-diagonal elements are very close to the full ones.
[25] K. Sturm and L. E. Oliveira, Phys. Rev. B **22**, 6268 (1980).
[26] F. Bechstedt, Phys. Status Solidi B **112**, 9 (1982).
[27] H. Suematsu and S. Tanuma, J. Phys. Soc. Jpn. **33**, 1619 (1972).